



Natural radioactivity and its radiological implications from soils and rocks in Jaintiapur area, North-east Bangladesh

Nafisa Tamannaya Dina¹ · Sudeb Chandra Das¹ · Mohammad Zafrul Kabir¹ · Md. Golam Rasul¹ · Farah Deeba¹ · Mohammad Rajib¹ · Md. Safiqul Islam¹ · Md. Abu Hayder² · Md. Idris Ali²

Received: 5 April 2022 / Accepted: 14 September 2022
© Akadémiai Kiadó, Budapest, Hungary 2022

Abstract

Natural radioactivity concentrations in recent alluvial soils from swampy areas and Tertiary rocks from Jaintiapur were measured using gamma-ray spectrometer equipped with HPGe detector. The average radioactivity concentration of ^{226}Ra , ^{232}Th and ^{40}K were 47 ± 6 , 64 ± 5 and $762 \pm 40 \text{ Bqkg}^{-1}$ in soils, whereas, 25 ± 2 , 37 ± 4 and $884 \pm 41 \text{ Bqkg}^{-1}$ in rock samples, respectively. Average radioactivity concentrations of studied soil and rock samples exceeded the world average except ^{226}Ra for rocks. Radio-elemental ratios suggest that an oxic depositional environment with low uranium and high thorium content. Regarding radiological hazard indices, radium equivalent activities (Ra_{eq}), external hazard index (H_{ex}) and internal hazard index (H_{in}) was found to be below the world permissible limits. Whereas, absorbed dose rate (D), and annual effective dose equivalent (AEDE) averages exceeded the world admissible values. Statistical studies show that radioactivity for ^{226}Ra and ^{232}Th linked to a source enriched in radioactive minerals and ^{40}K related to a different sources high in K enriched minerals.

Keywords Primordial radionuclides · Soil and rock · North-east Bangladesh · Radiological hazard · Gamma-spectrometry

Introduction

Human exposures are subjected to numerous degree of ionizing radiation from extra-terrestrial sources primarily include cosmic radiation from earth's outer atmosphere and terrestrial or naturally occurring radioactive sources such as gamma rays released from ^{40}K and radionuclides of ^{238}U and ^{232}Th through decay series present in soil, rocks and water [1–4]. Moreover, anthropogenic origins, such as weapon testing, nuclear treatment, nuclear incidents and nuclear power cycle are responsible for artificial radioisotopes in the environment. Natural and extra-terrestrial radiation exposure occur at various degrees in nature, and they differ regionally

caused by variation in geological and radiochemical properties in each region [5, 6].

Natural background radiation from primordial radionuclides such as ^{226}Ra , ^{232}Th , and ^{40}K in sediment, soil, water, and rock accounts for around 80% of the total radiation dosage a person receives in a year, making them the topic of most radioactivity measurement studies [7]. Of these, soil plays a major determinant of radioactive pollution in the environment because it operates as a means of transportation of radionuclide to biological systems [8]. In addition, soil radioactivity is frequently used to generate a benchmark for future radiation hazard analysis, nuclear safety, and exploration [9]. The distributions of ^{226}Ra , ^{232}Th , and ^{40}K in rock are influenced by the radionuclide distribution in parent rocks as well as the physicochemical processes that concentrate them. Higher levels of radiation are found in igneous rocks including dark colored heavy minerals, while lower levels of radiation are found in sedimentary rocks. The major sources of high natural background radiation are ^{238}U and its decay products in soils and rocks, as well as ^{232}Th in monazite sands [8]. Radioactive particles in phosphate rocks can reach the environment through a variety of methods, including the usage of phosphogypsum in construction and agriculture,

✉ Nafisa Tamannaya Dina
ashru.geo@gmail.com

✉ Sudeb Chandra Das
sudeb.geology@baec.gov.bd

¹ Institute of Nuclear Minerals, Bangladesh Atomic Energy Commission, Savar, Dhaka 1349, Bangladesh

² Health Physics and Radioactive Waste Management Unit, Institute of Nuclear Science and Technology, Bangladesh Atomic Energy Commission, Savar, Dhaka 1349, Bangladesh

as well as fertilization of agricultural fields [9]. Thus, through a systematic study of determination of the levels of different radionuclides (^{226}Ra , ^{232}Th and ^{40}K) and their associated health risks for human beings can act as a vital part in radiation protection, geo scientific studies and in establishing guidelines for the alleviation of these radionuclides [2]. Geologically, Bangladesh has already been categorized to four zones: (1) Eastern Mobile Belt (EMB), (2) Stable Platform (SP), (3) Dauki Fault Belt (DFB) and (4) Dinajpur Slope (DS) considering the favorable criteria of uranium formation [10]. A considerable amount of radiometric irregularities has subsequently been discovered in sandstone of Tipam and Dupitila Formations at the surrounding of Jaintiapur within the DFB zone. Moreover, this zone is found adjacent to the Mahadek uranium belt on the Shillong plateau's southern border. As a result, it's reasonable to believe that the uranium bearing solution has been streaming for a prolonged geologic period and that ore has accumulated within the DFB zone [10]. Geologically, Bangladesh is built up entirely of sedimentary rocks, and the ultimate prospect of uranium mineralization under favorable reducing conditions is sedimentary type uranium mineralization, which likely to be precipitated as economic uranium ore [10]. The reason for the study in this region of Jaintiapur is because the DFB zone has been demonstrated as potential area for uranium exploration, and data about natural radionuclides is currently lacking in this zone. Previous researches [10–13] have been focused to certain locations, radionuclides, and/or geological formations. As a result, a detailed analysis is highly needed to thoroughly estimate the dose of radiation exposure from environmental sources, the potentiality of uranium deposition, and assess the health concerns caused by radiation.

The purpose of this present work is to investigate the existence of natural ^{226}Ra , ^{232}Th and ^{40}K , and artificial ^{137}Cs radionuclide, as well as their activity concentration levels in the collected recent alluvial soils and Tertiary rocks samples from the geologic structure of Jaintiapur and the adjoining area of the DFB zone. Absorbed dose rate, radium equivalent, annual effective dose rate, as well as external and internal hazard index are calculated for estimating the radiological impact on the population and the environment related to these radionuclides. Additionally, these results are compared to values from other countries throughout the world as well as the UNSCEAR's reference value [6]. Therefore, the elemental concentration of these radionuclides, which provides information on the paleo-oxygenation condition of the investigated area, was calculated to find out the potentiality of uranium deposition. In addition, statistical studies are performed to understand the relationships between the radionuclide and radiation hazard indices. Moreover, this evaluation would serve as a reference data for assessing variations in environmental radiation.

Study area

The Bengal Basin is the northeastern part of Indian sub-continent bounded by the Precambrian Indian Shield platform in the west, the Precambrian Shillong Plateau in the north, Indo-Burman Ranges to the east and on the south it plunges in to the Bay of Bengal. The sedimentation of the Bengal Basin has been controlled by the movement and collision pattern of the Indian plate with the Burmese and Tibetan plates, as well as the uplift and erosion of the Himalayas and Indo Burman Ranges [14]. Surma Basins situated in the north-eastern part of Bangladesh (Fig. 1a), floored by an enormous thickness of sediments about 12 to 16 km from late Mesozoic to Cenozoic [15]. The Surma Basin is bordered to the north by the sole elevated topography, the Shillong Massif [16] (Fig. 1a). The contact between the Surma Basin and the Shillong Plateau is marked out by the E-W-trending Dauki Fault system with huge vertical displacement [15, 17]. The basin is bordered on the west by the Indian Shield Platform and on the east and southeast by the Chittagong–Tripura Fold Belt of the Indo-Burman Range [16] (Fig. 1a). The basin is open to the south and southeast to the Bengal Basin. Maximum number of litho-formations from the Eocene to recent is exposed in the Surma Basin. Stratigraphically, Sylhet Trough holds Tertiary Jaintia Group, Barail Group, Surma Group, Tipam Group, Dupi Tila Formation and Dihing Formation from older to younger [15, 18–20]. The possible source areas of the Surma Group sandstone may be the eastern Himalayan and/or from the Indo-Burman ranges and less commonly the Shillong Plateau [21].

The current research area, Jaintiapur and its surrounding areas in the Sylhet district, is located in Bangladesh's north eastern region (Fig. 1b). It covers Jaintiapur hill, Sripur Tea garden, Harafkata, Lalakhal Tea garden, as well as some bils and haors including Tama Bil, Kendri Bil, Yam Bil, Dibir haor and is located between longitude $92^{\circ}04'\text{E}$ – $92^{\circ}12'\text{E}$ and latitude $25^{\circ}04'\text{N}$ – $25^{\circ}16'\text{N}$.

Experimental

Sample collection and preparation

The soil and rock samples were taken from 13 randomly chosen points to determine the natural radioactivity concentration. The Location data of these sites were noted and defined as regards degree- minute- second (latitudinal and longitudinal position) with a hand held global positioning device (Model: Magellan-Map-410) units. For soil samples around 2 kg of soil was collected by removing the 5 cm

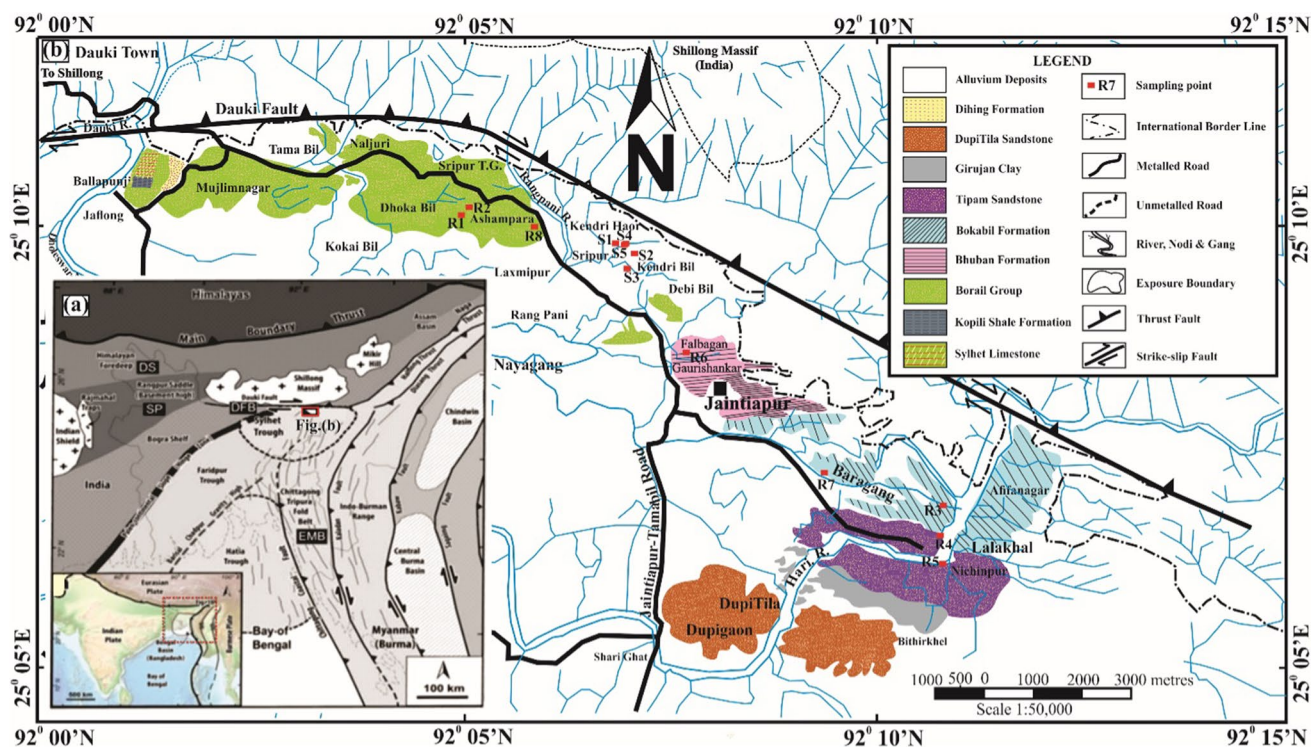


Fig. 1 a The regional geo-tectonic frameworks of the Bengal Basin (modified after [16, 22–24]) b Geological map of Jaintiapur and its adjoining areas showing the exposed geologic units and sample locations (modified after [12, 16])

surface soil. The rock samples were crushed to fine grains using a grinding machine after being cleaned and air dried. These samples were sieved with 2-mm mesh-sized sieve to produce homogeneous fine-sized particles and dried at 110 °C, over 24 h in a temperature-controlled furnace. The specimen was placed in an impervious 180 ml PVC container to avoid the get out of radiogenic gases radon (^{222}Rn) and thoron (^{220}Rn).

Sample counting and measurements

The radiological characterizations of the prepared samples were performed using γ -ray spectrometric analysis. The CANBERRA (Model GC-2018 and serial No. 0408941) spectrometer has a p-type coaxial high-purity germanium (HPGe) γ -ray detector of 93 cm³ active volume and 20% relative efficiency. The resolution of the detector was 2 keV (FWHM) at 1332 keV photo peak of ^{60}Co . A multichannel analyzer of 16 k was coupled with the detector. Genie-2000 spectra analysis software was operated to explain the spectra of all samples leading to determine the activity concentration. The energy regions selected for the corresponding radionuclides were 295.2 and 351.9 keV of ^{214}Pb ; 609.3 keV of ^{214}Bi for ^{226}Ra ; 238.6 and 300.1 keV of ^{212}Pb ; 583.2 keV of ^{208}Tl ; 911.1 and 969.1 keV of ^{228}Ac for ^{232}Th ; and 1460.8 keV for ^{40}K [25]. The activity concentrations of

^{40}K were calculated from its own γ -rays while the activity of ^{226}Ra and ^{232}Th was measured from the γ -rays of their decay products. In the spectrum no peak was available at energy of 661.6 keV, which is because of decay of ^{137}Cs [26].

Calibration of Gamma ray spectrometer

The detector's efficiency was calibrated with homogeneously integrated standard solutions of ^{226}Ra into inactive matrices (e.g., Al_2O_3). 180 ml Teflon container was used for formulating the standard source. A volume of the solution was pipetted into the matrices to generate the standard, which was then dried for 24 h at 408 °C [27]. Before measurement, the sample was thoroughly mixed to confirm that the radionuclides were uniformly distributed all across the source. The test uniformity was conducted on various aliquots of the ^{226}Ra solution mixed Al_2O_3 matrices [28, 29]. Figure 2 represents the efficiency calibration curve for solid matrix as a function of energy. Moreover, ^{137}Cs and ^{60}Co point source was used for the energy calibration of the detector.

The background radiation spectrum was used to calculate the lowest detectable activity of each radionuclide for the same counting time as for soil and rock samples and was estimated as 2.1, 4.2, and 59.1 Bqkg⁻¹ for ^{226}Ra , ^{232}Th , and ^{40}K respectively.

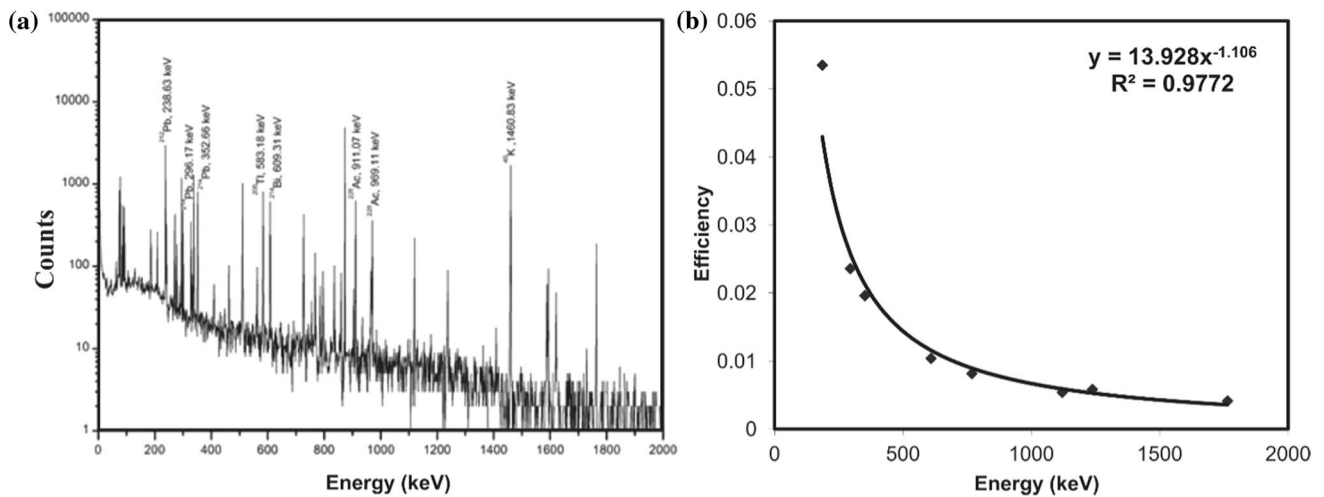


Fig. 2 a Energy diagram of the sample in HPGe detector with 20% efficiency b Efficiency curve of the HPGe detector in 4π geometry

Calculation of activity concentrations

The activity concentration (A) of each radionuclide in the studied samples was computed following equation [30]:

$$A = \frac{\text{cps} \times 1000}{E \times I \times W} \quad (1)$$

where, A = activity concentration in Bqkg^{-1} , cps = net counts per second, E = photo-peak efficiency I = gamma intensity and W = samples weight (in kg). The relative combined standard uncertainty (CSU) of the activity concentration was calculated (considering all known uncertainty components at coverage factor $k=1$) by using equation given below [31, 32]

$$\text{CSU} = \left(\frac{u(N)}{N} \right)^2 + \left(\frac{u(T)}{T} \right)^2 + \left(\frac{u(I\gamma)}{I\gamma} \right)^2 + \left(\frac{u(m)}{m} \right)^2 + \left(\frac{u(E)}{z} \right)^2 \quad (2)$$

where, N , T , $I\gamma$, m and E are the sample counts, counting time, gamma-ray emission probability, sample weight, and counting efficiency, respectively and $u(N)$, $u(T)$, $u(I\gamma)$, $u(m)$ and $u(E)$ are their respective uncertainties. In this study, the minimum detectable activity (MDA) of the gamma-ray measurement system was calculated by the following equation [33–35]

$$\text{MDA}(\text{Bqkg}^{-1}) = \frac{1.645\sqrt{B}}{E_{\text{eff}} \times I_{\gamma} \times w \times T} \quad (3)$$

where, B , is the background counts over the region of interest for each radionuclide and T , is the measurement time in seconds.

Radio-elemental ratios

The International Atomic Energy Agency [30] provides conversion factors to convert the measured ^{226}Ra , ^{232}Th , ^{40}K activity concentrations in Bqkg^{-1} to eU, eTh elemental concentrations in ppm and potassium in %. These recommended conversion factors are: 1 ppm U = 12.35 Bqkg^{-1} of ^{238}U ; 1 ppm Th = 4.06 Bqkg^{-1} of ^{232}Th ; and 1% K = 313 Bqkg^{-1} of ^{40}K . The ratio of eTh/eU activity concentration is important in identifying "geochemical faces." The viability of uranium to thorium ratio is employed as an indicator of relatively oxidizing or reduction circumstances based on examinations of several soil and sediment samples [36]. Under reducing circumstances, uranium has an immobile tetravalent phase that is stable, but it transforms into soluble hexavalent phase that can be transported in the solution. Thorium, on the other hand, has only one insoluble tetravalent form that is geochemically associated to uranium [37].

Radiological hazard

Radium equivalent activity concentration index (Ra_{eq})

Radium equivalent activity Ra_{eq} can be represented as the Eq. (4), the weighted summation of three radionuclides ^{226}Ra , ^{232}Th and ^{40}K [38]

$$\text{Ra}_{\text{eq}}(\text{Bqkg}^{-1}) = C_{\text{Ra}} + 1.43C_{\text{Th}} + 0.077C_{\text{K}} \quad (4)$$

Here, C_{Ra} , C_{Th} and C_{K} are the activity concentrations of ^{226}Ra , ^{232}Th and ^{40}K , respectively in Bqkg^{-1} .

Absorbed dose rate (D)

Absorbed dose rate (D) is calculated to assess the radiation exposure to gamma radiation at 1 m above the earth surface [39]

$$D(nGyh^{-1}) = 0.462C_{Ra} + 0.604C_{Th} + 0.0417C_K \quad (5)$$

Here C_{Ra} , C_{Th} and C_K are the activities of ^{226}Ra , ^{232}Th and ^{40}K in $Bqkg^{-1}$ and 0.462, 0.604 and 0.0417 are the conversion factors that convert the following activities in to doses [40].

The annual effective dose equivalent (AEDE)

AEDE was computed to estimate the health effects of the absorbed dose, which was calculated by using the following Eq. (6)

$$AEDE(mSvy^{-1}) = D \times DCF \times OF \times T \quad (6)$$

D is the absorbed gamma dose rate calculated in Eq. (3); According to UNSCEAR 2000, the DCF (dose conversion factor) and OF (outdoor occupancy factor) values are $0.7 SvGy^{-1}$ and 0.2, respectively, as well as T is the time factor (8760 h). $OF=0.2$ was derived from the assumption that human roughly spend 20% time outside [41].

External hazard index

The external and internal hazard indexes was calculated to make sure that radiation exposure due to ^{226}Ra , ^{232}Th and ^{40}K in the analyzed samples are within the allowable dose equivalent of $1 mSvy^{-1}$ [38]. Equation (7) is used to determine the external hazard index.

$$H_{ex} = (C_{Ra}/370 + C_{Th}/259 + C_K/4810) \leq 1 \quad (7)$$

Internal hazard index

Internal hazard index (H_{in}) was calculated using the following formula (8): [42],

$$H_{in} = (C_{Ra}/185 + C_{Th}/259 + C_K/4810) \leq 1 \quad (8)$$

Here, C_{Ra} , C_{Th} and C_K having the same meaning as in Eq. (4). Radiation hazard are considered insignificant when the value of this index value is lower than 1.

Statistical analysis

Statistical studies including Pearson correlation coefficient analysis, and Principal component analysis were

performed with SPSS (version 23) to understand the overall relationships between the combinations of radionuclides and the variables derived from activity concentration, with a view to notice the magnitude of the existence of these radionuclides collectively in positive vicinity.

Results and discussion

Activity concentrations

The activity concentrations of ^{226}Ra , ^{232}Th and ^{40}K computed in $Bqkg^{-1}$ for all samples are presented in Table. 1. ^{226}Ra activity concentrations ranged from 22 ± 2 to $66 \pm 2 Bqkg^{-1}$ (soil samples) with an average activity of $47 \pm 6 Bqkg^{-1}$ and from 14 ± 2 to $51 \pm 2 Bqkg^{-1}$ (rock samples) with an average activity of $25 \pm 2 Bqkg^{-1}$. For ^{232}Th the values ranged from 25 ± 3 to $92 \pm 4 Bqkg^{-1}$ (soil samples) with an average activity of $64 \pm 5 Bqkg^{-1}$ and from 20 ± 3 to $57 \pm 3 Bqkg^{-1}$ (rock samples) with an average activity of $37 \pm 4 Bqkg^{-1}$. The activity concentrations for ^{40}K ranged from 408 ± 34 to $1006 \pm 40 Bqkg^{-1}$ (soil samples) with an average activity of $762 \pm 40 Bqkg^{-1}$ and from 544 ± 36 to $2060 \pm 54 Bqkg^{-1}$ (rock samples) with an average activity of $884 \pm 41 Bqkg^{-1}$ (Table 1). The special distribution map represented the activity concentrations of all radionuclides detected in the analyzed samples (Fig. 3). The higher concentration of ^{226}Ra and ^{232}Th is mainly found in the soil samples, whereas R-7 rock sample shows higher ^{40}K concentrations (Fig. 3). The average activity concentration was followed an ascending order as $^{226}Ra < ^{232}Th < ^{40}K$. In all of the studied soil and rock samples, ^{40}K activity was usually the largest contributor to the particular activity when compared to ^{232}Th and ^{226}Ra . The world's average activity concentrations for ^{226}Ra , ^{232}Th and ^{40}K are accordingly 35, 30, and 400 $Bqkg^{-1}$ [6]. The average activity concentration values of ^{232}Th and ^{40}K for both the soil and rock samples of the studied area were greater than the world's average values [6], while the mean concentration of ^{226}Ra was higher compare to the world's average values for soil, however, the value for rock samples lie within the limit. In comparison to the mean activity concentration of ^{226}Ra and ^{232}Th for rock samples, it was higher in soil samples from the research area. Moreover, the studied confirmed the absence of artificial ^{137}Cs radionuclide, the activity concentrations of all the analyzed samples were found beneath the minimum detection limit of $0.18 Bqkg^{-1}$ (Table 1).

Heavy minerals are incorporated with ^{226}Ra and ^{232}Th radionuclides in their crystal structure whereas light minerals like quartz and feldspar can have comparatively high quantities of ^{40}K [43]. Heavy minerals might be present at sample locations with high ^{226}Ra and ^{232}Th concentrations, while light minerals might be present in sampling

Table 1 Activity concentrations of ^{226}Ra , ^{232}Th and ^{40}K , absorbed dose rate (D), annual effective dose equivalent (AEDE), radium equivalent activity (Ra_{eq}), external (H_{ex}), and internal (H_{in}) hazard index in soil and rock samples from Jaintiapur area as well as comparison of this studies with other areas of Bangladesh and worldwide

Sample ID	Sample Type	^{226}Ra (Bqkg $^{-1}$)	^{232}Th (Bqkg $^{-1}$)	^{40}K (Bqkg $^{-1}$)	^{137}Cs (Bqkg $^{-1}$)	Ra_{eq} (Bqkg $^{-1}$)	H_{ex}	H_{in}	D (nGyh $^{-1}$)	AEDE (mSvy $^{-1}$)
<i>Soil</i>										
S-1	Alluvial Soil	55 ± 3	83 ± 6	750 ± 40	Below detection limit (0.18)	231	0.62	0.77	107	0.13
S-2	Alluvial Soil	66 ± 2	92 ± 4	1006 ± 40		274	0.74	0.92	128	0.16
S-3	Alluvial Soil	54 ± 3	59 ± 6	847 ± 46		204	0.55	0.70	96	0.12
S-4	Alluvial Soil	37 ± 20	61 ± 4	799 ± 41		186	0.50	0.60	88	0.11
S-5	Alluvial Soil	22 ± 2	25 ± 3	408 ± 34		88	0.24	0.30	42	0.05
Maximum		66 ± 2	66 ± 2	92 ± 4		1006 ± 40	274	0.74	0.92	128
Minimum		22 ± 2	22 ± 2	25 ± 3	408 ± 34	88	0.24	0.60	42	
Average		47 ± 6	64 ± 5	762 ± 40	197	0.53	0.66	92	0.11	
<i>Rock</i>										
R-1	Barail Sandstone	24 ± 2	39 ± 3	600 ± 36		125	0.34	0.40	60	0.07
R-2	Barail Sandstone	14 ± 1	20 ± 2	544 ± 36		83	0.23	0.26	41	0.05
R-3	Bokabil Sandstone	27 ± 2	39 ± 5	565 ± 42		126	0.34	0.42	60	0.07
R-4	Tipam Sandstone	24 ± 2	28 ± 5	907 ± 44		133	0.36	0.42	66	0.08
R-5	Tipam Sandstone	14 ± 2	23 ± 3	873 ± 41		114	0.31	0.35	57	0.07
R-6	Bhuban Shale	51 ± 2	57 ± 3	872 ± 40		200	0.54	0.68	95	0.12
R-7	Bokabil Sandstone	19 ± 2	54 ± 4	2060 ± 54		255	0.69	0.74	128	0.16
R-8	Barail Sandstone	24 ± 2	36 ± 3	654 ± 38		126	0.34	0.41	61	0.07
Maximum		51 ± 2	51 ± 2	57 ± 3		2060 ± 54	255	0.69	0.74	128
Minimum		14 ± 1	14 ± 2	20 ± 2		544 ± 36	83	0.23	0.26	41
Average		25 ± 2	37 ± 4	884 ± 41		145	0.39	0.46	71	0.09
World average [6]		35	30	400		370	1	1	55	0.07
Inani Beach [51]		44	70	1007		222	0.60	0.72	105	0.13
Chittagong [11]		35	60	438		154	0.42	0.51	71	0.09
Pabna [52]		33	47	449		135	0.36	0.45	62	0.08
Dhaka [53]		33	55	574		156	0.42	0.51	73	0.09
Jessore [54]		48	53	481		161	0.43	0.56	74	0.09
Sitakunda [55]		31	62	467		155	0.42	0.50	71	0.09
Sylhet [11]		55	125	491		271	0.73	0.88	122	0.15
Habiganj [13]		11	22	227		60	0.16	0.19	28	0.03
Egypt [56]		17	18	320		67	0.18	0.23	32	0.04
USA [6]		40	35	370		118	0.32	0.43	55	0.07
China [57]		32	41	440		124	0.34	0.42	58	0.07
Japan [6]		33	28	310		97	0.26	0.35	45	0.06
Malaysia [58]		66	82	310		207	0.56	0.74	93	0.11
India [59]		29	64	400		151	0.41	0.49	69	0.08
Iran [6]		28	22	640		109	0.29	0.37	53	0.07
Saudi Arabia [60]		15	11	225		48	0.13	0.17	23	0.03
Turkey [61]		86	51	772		218	0.59	0.82	103	0.13

locations with high ^{40}K concentrations. The probable reasons for higher activity concentration in soil include presence of higher organic matter content, dominance of minerals (smectite, clays, and carbonates), the difference in the underlying bedrocks, and the inundation of these area during flooding through several streams and channels flown through

the different formations exposed in nearby highly radioactive Khasi and Jaintia hills of Shillong Plateau, Meghalaya, India and Tertiary succession of Jaintiapur Area of Surma basin which carry various sediments from different formations having diverse age range [12, 44, 45]. The activities of radionuclides in the soil samples may vary locally even in

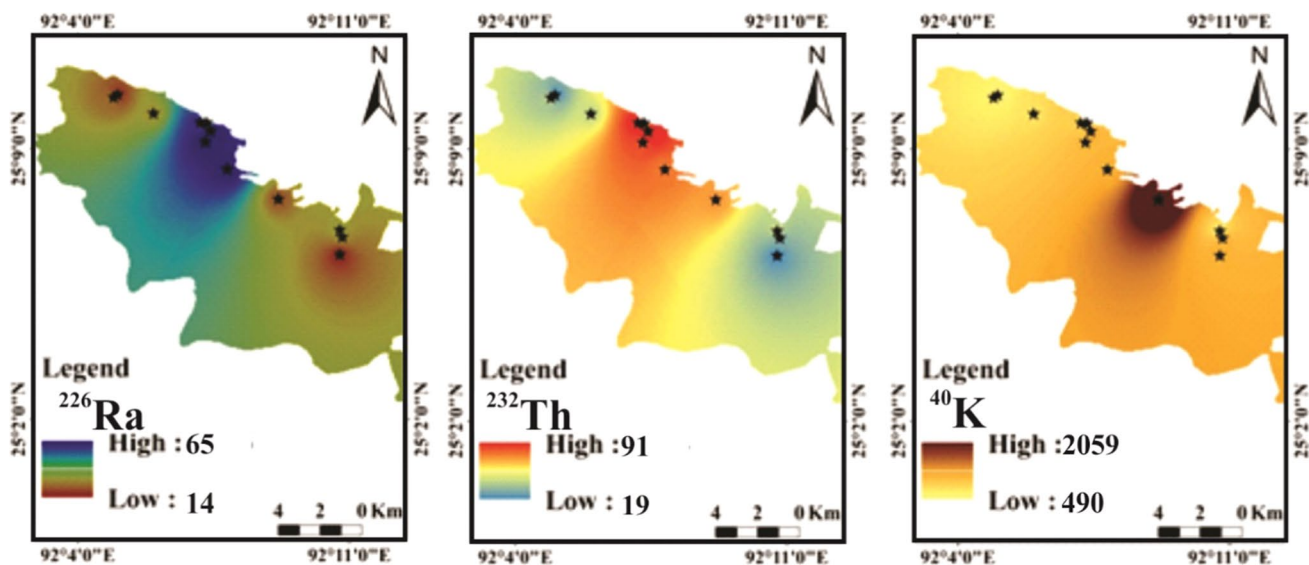


Fig. 3 Spatial distribution map of ^{226}Ra , ^{232}Th and ^{40}K activity concentrations (BqKg^{-1}) in the study area

shorter distance due to multi-channel sediments deposition which we have observed during in-situ field measurements. Similar studies from Shillong Plateau, Meghalaya, India also showed that the variation of the radioactivity content from location to location is because of the variation of these elements in different geological formations of oldest Precambrian gneissic complex to Recent alluvium soil [46, 47]. Therefore, the reasons for fluctuating activity concentrations in the studied area include the variation of mineralogical and chemical composition of rock formations exposed in the studied area which were deposited in varied depositional settings such as continental to marine in the geological past, the presence or absence of alluvium covering and compactness of sandstone [12, 16, 48]. A close observation during the field survey revealed that black patches on the soils indicating the presence of thorium in the studied samples and the variation arises due to varying grades of monazite deposition in the samples. These were further confirmed from the previous mineralogical studies of this area available in literatures [16, 48–50]. Previous XRD analysis of Neogene Surma Group sedimentary rocks from the current study area confirmed the presence of kaolinite, illite, chlorite, illite/smectite and kaolinite/smectite mixed layers. Petrographic studies show that sandstones consist dominantly quartz (61%), feldspar (8%) with lithic fragments (12%) and the shales contain mainly quartz, feldspar and clay minerals with minor carbonates. In Meghalaya, the uranium containing host rock is feldspar rich Arkosic sandstone and the thorium containing host rock contain monazite [46]. Besides, the anthropogenic activities such as use of fertilizer containing potassium in the haor and bills area during agricultural activities and presence of stone crushing site nearby the studied area might result in

variation of activity concentrations [3, 12, 45]. Thus, there is no significant correlation exist between radionuclides in soil samples and activity of radionuclides in rock samples of the study area.

Mean activity concentration of ^{226}Ra , ^{232}Th and ^{40}K in studied area was compared with the mean activity concentration of soil from different parts of Bangladesh and with different countries of the world (Table 1). Where the average values of ^{226}Ra , ^{232}Th and ^{40}K in samples were within the range or exceed the respective values of the countries listed.

Radio-elemental concentration with ratios

The calculated uranium and thorium concentration in ppm and potassium in weight % is shown in (Table 2). Uranium concentration varied from (1.7 to 5.3) ppm and (1.1 to 4.1) ppm and Thorium concentration was in the range of (6.06 to 22.6) ppm and (4.8 to 14) ppm for soil and rock samples respectively, ^{40}K concentration was in the range of (1.3 to 3.2) % and (1.7 to 6.5) % for soil and rock samples. The elemental concentration of uranium and thorium in soil samples were just exceed the average UCC value [62]. In contrast, potassium % in rock samples largely exceed the UCC value. The radioactive minerals could be the cause of higher value of radioactivity concentrations of the studied samples.

The eU/eTh ratio was being used as a redox indicator with a view to determine the paleo-oxygenation status of the studied deposits. A eU/eTh ratio less than 1.25 indicates oxic depositional conditions, as well as ratio more than 1.25 indicates sub-oxic and anoxic conditions [63–65]. In the present study, average eU/eTh ratio is 0.24 and 0.22 for soil and rock

Table 2 Elemental concentrations of Uranium, Thorium (ppm), Potassium (%) and elemental ratio of eU/eTh, eTh/eU, in soil and rock samples

Sample ID	U (ppm)	Th (ppm)	K%	eU/eTh	eTh/eU
S-1	4.47	20.37	2.39	0.22	4.56
S-2	5.32	22.61	3.21	0.24	4.25
S-3	4.38	14.57	2.71	0.3	3.33
S-4	2.99	15.09	2.55	0.2	5.05
S-5	1.77	6.07	1.3	0.29	3.43
Maximum	5.32	22.61	3.21	0.3	5.05
Minimum	1.77	6.07	1.3	0.2	3.33
Average	3.79	15.74	2.43	0.25	4.12
R-1	1.91	9.61	1.92	0.2	5.03
R-2	1.11	4.82	1.74	0.23	4.34
R-3	2.2	9.6	1.81	0.23	4.35
R-4	1.92	6.78	2.9	0.28	3.53
R-5	1.12	5.64	2.79	0.2	5.02
R-6	4.15	14.01	2.78	0.3	3.37
R-7	1.54	13.37	6.58	0.11	8.71
R-8	1.94	8.96	2.09	0.22	4.61
Maximum	4.15	14.01	6.58	0.3	8.71
Minimum	1.11	4.82	1.74	0.11	3.37
Average	1.99	9.1	2.83	0.22	4.87
UCC [47]	2.7	10.5	2.8	0.26	3.89

samples respectively, which suggesting the samples were deposited in an oxic environment.

eTh/eU ratio < 2 implies relative uranium enrichment and the presence of reducing conditions. The intermediate (2 to 7) facies is assumed to suggest poor weathering and quick deposition of igneous rock debris, as well as eTh/eU > 7, which indicate the eliminations of favorable enrichment, possibly due to leaching [36]. In the present study, Table 2 shows a wide range of eTh/eU ratio (3.32 to 5.05) for soil samples and (3.37 to 8.71) for rock samples. The average eTh/eU ratio was 4.12 for soil samples and 4.87 for rock samples which exceed the average UCC value (3.8) [66, 67], indicating intermediate to high facies, suggesting poor weathering and quick deposition of igneous rock detritus and low uranium content over the crust composition and both soil and rock samples are enriched in Th.

Radiological hazards

The measured Ra_{eq} (Table 1) was ranges from 204 to 274 $Bqkg^{-1}$ and 126 to 133 $Bqkg^{-1}$ with an average of 236 and 130 $Bqkg^{-1}$ for soil and rock samples. Average Ra_{eq} value was below the maximum admissible value of 370 $Bqkg^{-1}$ [4].

The estimated absorbed dose rates listed in (Table 1), range from 96 to 128 $nGyh^{-1}$ and 60 to 65 $nGyh^{-1}$ with the

average values of 110 $nGyh^{-1}$ and 63 $nGyh^{-1}$ for soil and rock samples and this values exceed the accepted limit 55 $nGyh^{-1}$ [4]. Absorbed dose rates vary according with the spatial variations of activity concentrations of radionuclide in minerals of soil and rock shown in (Fig. 4). Absorbed dose rates are found highest in S-2 location where ^{226}Ra and ^{232}Th concentrations are highest, and in R- 7 location the ^{40}K concentrations is also reached to highest of the study.

The outdoor annual effective dose equivalent values (Table 1) varied from 0.01 to 0.15 $mSvy^{-1}$ and 0.05 to 0.157 $mSvy^{-1}$ for soil and rock samples, respectively, with average of 0.113 $mSvy^{-1}$ and 0.086 $mSvy^{-1}$. The values for both soil and rock samples are somewhat exceed the world wide average of 0.07 $mSvy^{-1}$ for outdoor annual effective dose [6].

External hazard index (Table 1) values for soil and rock samples varied from 0.55 to 0.74, and 0.34 to 0.35, including a mean of 0.63 and 0.35, whereas internal hazard index values for soil and rock samples ranged from 0.60 to 0.91 and 0.20 to 0.74, with a mean of 0.65 and 0.45. The hazard indexes were below the world permissible value 1 [6].

Statistical analysis

Pearson's correlation coefficient analysis

Pearson correlation coefficient analysis has been used as a bivariate statistic to evaluate the mutual relationships and strength of the association between pairs of variables [68]. Pearson correlation coefficients among radionuclides and radiological hazard indices for all the studied samples are presented in Table 3. There is a strong positive statistical relationship between ^{232}Th and ^{238}U in all hazard indices Ra_{eq} , H_{ex} , H_{in} , D , and $AEDE$ with a P value < 0.02. A significant positive statistical relationship is observed between ^{226}Ra and ^{232}Th with correlation coefficient equals 0.891 because uranium and thorium decay series arise simultaneously [69]. In contrast, ^{40}K showed a very weak correlation with ^{226}Ra and ^{232}Th ($Bqkg^{-1}$), would be related to the high potassium solubility [70]. The competing chemical properties could affect the adsorption of these ions on clay particle and describe the association of ^{40}K with ^{226}Ra and ^{232}Th series [71]. Furthermore, ^{40}K has a strong positive correlation with D , and $AEDE$. Therefore, it can be presumed that, all the radionuclides ^{226}Ra , ^{232}Th and ^{40}K , influence to the gamma emission in all places.

Principal component analysis

Factor analysis is a statistical tool for determining interconnections between radioactive variables and describing them in regards of their common underlying dimensions (factors) [72]. Only factors with eigenvalues greater than 1 are taken

Fig. 4 Absorbed dose rates due to the natural radioactivity in different samples sites of the study area

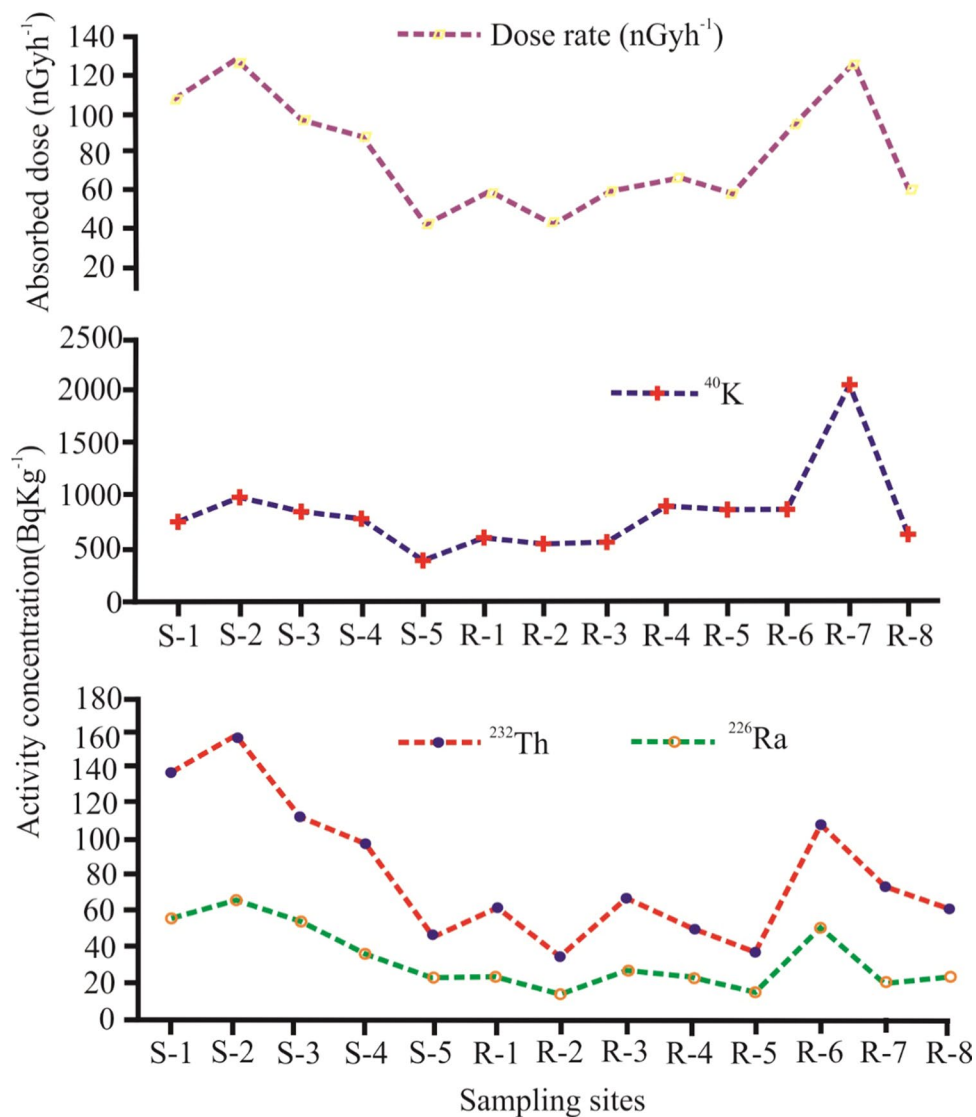


Table 3 Pearson correlation coefficients between radioactive variables in studied samples

Variables	²³⁸ U	²³² Th	⁴⁰ K	Ra _{eq}	H _{ex}	H _{in}	D	AEDE
²³⁸ U	1							
²³² Th	0.891**	1						
⁴⁰ K	0.019	0.313	1					
Ra _{eq}	0.744**	0.915**	0.658*	1				
H _{ex}	0.741**	0.912**	0.663*	1.000**	1			
H _{in}	0.838**	0.951**	0.543	0.988**	0.987**	1		
D	0.692**	0.879**	0.718**	0.997**	0.997**	0.973**	1	
AEDE	0.691**	0.871**	0.723**	0.994**	0.995**	0.971**	0.999**	1

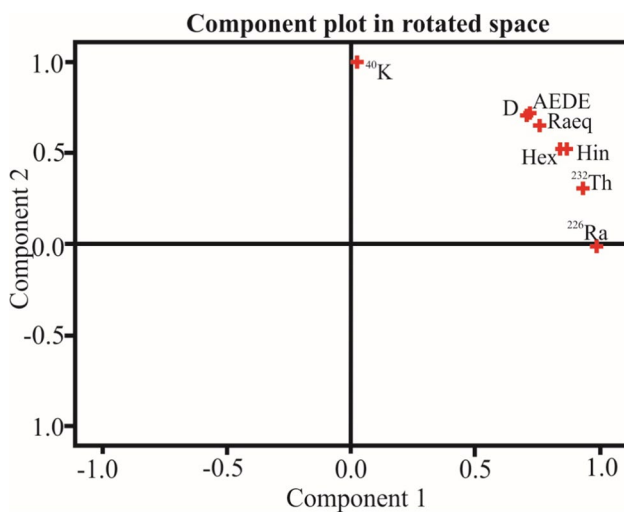
* Correlation is significant at the 0.05 level (2-tailed)
 ** Correlation is significant at the 0.01 level (2-tailed)

into account. Table 4 represents the varimax rotated factor loadings, including the eigen values and eigen communalities. The findings revealed that there were two eigen values greater than one, implying that these two elements could be

related over 99.27% of the total variance is explained. PC1 accounted for 86.49% of the overall variation and all the hazard parameters originated from ²³²Th and ²³⁸U series are significantly loaded. The second component PC2, loaded with

Table 4 Rotated factor loadings of PCA 1 and PCA 2

Variables	Component	
	1	2
^{238}U	0.987	-0.009
^{232}Th	0.936	0.306
^{40}K	0.019	0.998
Ra_{eq}	0.763	0.646
H_{ex}	0.759	0.650
H_{in}	0.850	0.526
D	0.708	0.706
AEDE	0.703	0.710
Eigen value	7.780	1.150
Variance explained in%	86.49%	12.77%

**Fig. 5** Rotated factor loadings of PCA 1 (86.49%) and PCA 2 (12.77%)

potassium and radiological hazard effects (D, and AEDE), which explain 12.779% percent of the total variance. The rotating factor loading of radiological parameters is shown in Fig. 5.

Conclusions

The radioactivity concentration of primordial ^{226}Ra , ^{232}Th , and ^{40}K radionuclides was analyzed using a gamma-ray spectrometer for soil and rock samples collected from Swampy land and adjacent area of Jaintiapur, Sylhet, Bangladesh. The mean activity concentrations of ^{232}Th and ^{40}K in the studied soil and rock samples, as well as ^{226}Ra in soil, were all above the world permissible value [6]. Whereas, the measured mean activity of ^{226}Ra for rocks samples was within the world admissible levels of 35. The extracted

values were, in general, higher than international reference value, however corresponding to other countries of the world didn't significantly vary. Radiological safety impact parameters inclusive of estimated average values of Ra_{eq} as well as H_{ex} and H_{in} were less than the sort of international reference value [6]. In radiological hazards analysis, absorbed dose rate D, and AEDE in studied samples were found exceed the standard limits for radiological safety. The processed statistical methods were also confirmed that these D, and AEDE are comes from both ^{232}Th , ^{226}Ra series and ^{40}K series. This suggests that local residents of the studied area are exposed to radiation, indicating the need for further research in this area. Elemental eU/eTh and eTh/eU ratios indicated an oxic depositional environment, along with low uranium and high thorium concentration. So, further investigation is still needed to find out the potentiality of uranium deposition in this studied area of Dauki Fault Belt (DFB) zone. Moreover, this research work might be applicable for natural radioactivity mapping and will establish a reference data for future assessment of the surroundings of Jaintiapur.

Acknowledgements The authors of this paper are sincerely thankful to the scientific and technical personnel of the Institute of Nuclear Minerals of the Bangladesh Atomic Energy Commission for the help during field excursion. The contribution in the field work by the deceased Dr. Mohammad Ibrahim Khalil due to Covid 19 is greatly acknowledged and prayed for his soul to rest in peace. Sincere acknowledgement goes to the local people and administration for their logistic help and cooperation in the field. Constructive suggestions of the anonymous reviewers are gratefully appreciated. Authors sincerely acknowledge the editor, Zsolt Revay for his valuable suggestions to improve the manuscript.

Author contributions Conceptualization and writing-original draft, data curation, map preparation, [NTD]; writing and review, data analysis, map preparation [SCD]; field investigation, review & editing, [MK]; funding acquisition, review & editing, [GR]; review & editing, [FD & MR]; field investigation, [SI]; Laboratory analysis, [AH & IA]. All authors have read and agreed to the published version of the manuscript.

Funding We confirm that this work is original and has not been published elsewhere nor it currently under consideration for publication elsewhere. All authors of this research paper have directly participated in the planning, execution, or analysis of this study. All authors have seen and approved the final version of the manuscript being submitted. To the best of our knowledge, no conflict of interest, financial or other, exists.

Declarations

Conflict of interest The authors declare that they have no known competing financial interests or personal relationships that could have appeared to influence the work reported in this paper.

References

- Arıman S, Gümüş H (2018) Radioactivity levels and health risks due to radionuclides in the soil and sediment of mid-Black Sea:

- kizilirmak Deltas-Turkey. *Radiochim Acta* 106:927–937. <https://doi.org/10.1515/ract-2017-2896>
2. Prasad M, Ranga V, Kumar GA, Ramola RC (2020) Radiological impact assessment of soil and groundwater of Himalayan regions in Uttarakhand, India. *J Radioanal Nucl Chem* 323:1269–1282. <https://doi.org/10.1007/s10967-019-06827-9>
 3. Tawfic A, Zakaly HM, Awad HA et al (2021) Natural radioactivity levels and radiological implications in the high natural radiation area of Wadi El Reddah. *Egypt J Radioanal Nucl Chem* 327:643–652
 4. UNSCEAR (1988) Sources, effects and risks of ionizing radiation: 1988 report to the General Assembly, with annexes. United Nations, New York
 5. Özdemir Öge T, Özdemir FB, Öge M (2021) Assessment of environmental radioactivity in soil samples from Bartın Province, Turkey. *J Radioanal Nucl Chem* 328:149–162. <https://doi.org/10.1007/s10967-021-07629-8>
 6. UNSCEAR (2000) Sources and effects of ionizing radiation, ANNEX B, Exposures from natural radiation sources. UNSCEAR 2000 REPORT. N Y 1:97–99
 7. Al-Jundi J, Al-Bataina BA, Abu-Rukah Y, Shehadeh HM (2003) Natural radioactivity concentrations in soil samples along the Amman Aqaba Highway, Jordan. *Radiat Meas* 36:555–560. [https://doi.org/10.1016/S1350-4487\(03\)00202-6](https://doi.org/10.1016/S1350-4487(03)00202-6)
 8. Al-Hamarneh IF, Awadallah MI (2009) Soil radioactivity levels and radiation hazard assessment in the highlands of northern Jordan. *Radiat Meas* 44:102–110. <https://doi.org/10.1016/j.radmeas.2008.11.005>
 9. Ramli AT, Hussein AWMA, Wood AK (2005) Environmental ²³⁸U and ²³²Th concentration measurements in an area of high level natural background radiation at Palong, Johor, Malaysia. *J Environ Radioact* 80:287–304. <https://doi.org/10.1016/j.jenvrad.2004.06.008>
 10. Majumder R, Khalil M, Rashid M (2014) Uranium exploration status in Bangladesh: Conceptual feasibility studies. 1
 11. Chowdhury MI, Alam MN, Hazari SKS (1999) Distribution of radionuclides in the river sediments and coastal soils of Chittagong, Bangladesh and evaluation of the radiation hazard. *Appl Radiat Isot* 51:747–755. [https://doi.org/10.1016/S0969-8043\(99\)00098-6](https://doi.org/10.1016/S0969-8043(99)00098-6)
 12. Majumder RK, Das SC, Rasul MdG et al (2021) Measurement of radon concentrations and their annual effective doses in soils and rocks of Jaintiapur and its adjacent areas, Sylhet, North-east Bangladesh. *J Radioanal Nucl Chem* 329:265–277. <https://doi.org/10.1007/s10967-021-07771-3>
 13. Rahman MM, Rahman R, Hasan S, Ferdous N (2015) Radioactivity Distributions in Soils from Habiganj District, Bangladesh and their Radiological Implications. 19:13
 14. Alam M (1989) Geology and depositional history of Cenozoic sediments of the Bengal Basin of Bangladesh. *Palaeogeogr Palaeoclimatol Palaeoecol* 69:125–139
 15. Johnson SY, Nur Alam AMd (1991) Sedimentation and tectonics of the Sylhet trough, Bangladesh. *GSA Bull* 103:1513–1527. [https://doi.org/10.1130/0016-7606\(1991\)103%3c1513:SATOTS%3e2.3.CO;2](https://doi.org/10.1130/0016-7606(1991)103%3c1513:SATOTS%3e2.3.CO;2)
 16. Khanam F, Rahman MJJ, Alam MM, Abdullah R (2021) Sedimentology and basin-fill history of the Cenozoic succession of the Sylhet Trough, Bengal Basin, Bangladesh. *Int J Earth Sci (Geol Rundsch)* 110:193–212. <https://doi.org/10.1007/s00531-020-01946-1>
 17. Hiller K, Elchi M (1984) Structural development and hydrocarbon entrapment in the Surma Basin/Bangladesh (Northwest Indo Burman Fold Belt). p SPE-12398-MS
 18. Evans P (1932) Tertiary succession in Assam. *Trans Min Geol Inst India* 27:155–260
 19. Holtrop J, Keizer J (1970) Some aspects of the stratigraphy and correlation of the Surma Basin wells, East Pakistan. *ECAFE Miner Resour Dev Ser* 36:143–154
 20. Reimann K-U, Hiller K (1993) Geology of Bangladesh
 21. Uddin A, Lundberg N (1998) Cenozoic history of the Himalayan-Bengal system: sand composition in the Bengal basin, Bangladesh. *Geol Soc Am Bull* 110:497–511
 22. Abdullah R, Yeasmin R, Mahbulul Ameen SM et al (2015) 2D structural modelling and hydrocarbon potentiality of the Sitakund structure, Chittagong Tripura Fold Belt, Bengal Basin, Bangladesh. *J Geol Soc India* 85:697–705. <https://doi.org/10.1007/s12594-015-0266-8>
 23. Alam M, Alam MM, Curray JR et al (2003) An overview of the sedimentary geology of the Bengal Basin in relation to the regional tectonic framework and basin-fill history. *Sed Geol* 155:179–208. [https://doi.org/10.1016/S0037-0738\(02\)00180-X](https://doi.org/10.1016/S0037-0738(02)00180-X)
 24. Hossain MdS, Khan MdSH, Chowdhury KR, Abdullah R (2019) Synthesis of the Tectonic and Structural Elements of the Bengal Basin and Its Surroundings. In: Mukherjee S (ed) *Tectonics and Structural Geology: Indian Context*. Springer, Cham, pp 135–218
 25. Roessler CE, Smith ZA, Bolch WE, Prince RJ (1979) Uranium and radium-226 in florida phosphate materials. *Health Phys* 37:269–277. <https://doi.org/10.1097/00004032-197909000-00001>
 26. El-Tahawy M, Farouk M, Hammad F, Ibrahim N (1992) Natural potassium as a standard source for the absolute efficiency calibration of Ge detectors. *J Nucl Sci* 29:361–363
 27. Harb S, Salahel Din K, Abbady A (2008) Study of efficiency calibrations of HPGe detectors for radioactivity measurements of environmental samples
 28. Hossain MK, Hossain SM, Azim R, Meaze AMH (2010) Assessment of radiological contamination of soils due to shipbreaking using HPGe digital gamma-ray spectrometry system. *J Environ Prot* 1:10
 29. Islam SS, Ali MI, Haydar M et al (2017) Background gamma radiation mapping in forest ecosystem of Bangladesh: a study on the radioactivity distribution in the national reserve forest of Gazipur. *Radiat Prot Environ* 40:73
 30. IAEA (1989) Construction and use of calibration facilities for radiometric field equipment. Internat. Atomic Energy Agency
 31. Asaduzzaman K, Khandaker MU, Amin YM, Bradley DA (2016) Natural radioactivity levels and radiological assessment of decorative building materials in Bangladesh. *Indoor Built Environ* 25:541–550. <https://doi.org/10.1177/1420326X14562048>
 32. Haydar MA, Hasan MM, Jahan I et al (2021) The status of NORMs in natural environment adjacent to the Rooppur nuclear power plant of Bangladesh. *Nucl Eng Technol* 53:4114–4121. <https://doi.org/10.1016/j.net.2021.06.025>
 33. Khandaker MU, Jojo PJ, Kassim HA, Amin YM (2012) Radiometric analysis of construction materials using HPGe gamma-ray spectrometry. *Radiat Prot Dosim* 152:33–37. <https://doi.org/10.1093/rpd/ncs145>
 34. Khandaker MU, Mohd Nasir NL, Asaduzzaman K et al (2016) Evaluation of radionuclides transfer from soil-to-edible flora and estimation of radiological dose to the Malaysian populace. *Chemosphere* 154:528–536. <https://doi.org/10.1016/j.chemosphere.2016.03.121>
 35. Khandaker MU, Asaduzzaman K, Sulaiman AFB et al (2018) Elevated concentrations of naturally occurring radionuclides in heavy mineral-rich beach sands of Langkawi Island, Malaysia. *Mar Pollut Bull* 127:654–663. <https://doi.org/10.1016/j.marpolbul.2017.12.055>
 36. Adams JA, Weaver CE (1958) Thorium-to-uranium ratios as indicators of sedimentary processes: example of concept of geochemical facies. *AAPG Bull* 42:387–430

37. Doveton JH, Prensley SE (1992) Geological applications of wireline logs: a synopsis of developments and trends. *Log Anal* 33:286–303
38. Beretka J, Mathew PJ (1985) Natural radioactivity of Australian building materials. *Ind Wastes By-prod Health Phys* 48:87–95. <https://doi.org/10.1097/00004032-198501000-00007>
39. UNSCEAR (2008) Sources and effects of ionizing radiation, UNSCEAR 2008 report. United Nations, New York
40. Uosif MAM (2011) Specific Activity of ²²⁶Ra, ²³²Th and ⁴⁰K for Assessment of Radiation Hazards from Building Materials Commonly Used in Upper Egypt. 8
41. Debertin K, Helmer RG (1988) Gamma-and X-ray spectrometry with semiconductor detectors
42. Ramasamy V, Suresh G, Meenakshisundaram V, Ponnusamy V (2011) Horizontal and vertical characterization of radionuclides and minerals in river sediments. *Appl Radiat Isot* 69:184–195. <https://doi.org/10.1016/j.apradiso.2010.07.020>
43. Carvalho C, Anjos R, Veiga R, Macario K (2011) Application of radiometric analysis in the study of provenance and transport processes of Brazilian coastal sediments. *J Environ Radioact* 102:185–192
44. Cumberland SA, Douglas G, Grice K, Moreau JW (2016) Uranium mobility in organic matter-rich sediments: a review of geological and geochemical processes. *Earth Sci Rev* 159:160–185
45. Jananee B, Rajalakshmi A, Thangam V et al (2021) Natural radioactivity in soils of Elephant hills, Tamilnadu, India. *J Radioanal Nucl Chem* 329:1261–1268. <https://doi.org/10.1007/s10967-021-07886-7>
46. War SA, Nongkynrih P, Khathing DT et al (2008) Spatial distribution of natural radioactivity levels in topsoil around the high-uranium mineralization zone of Kylleng-Pyndensohiong (Mawthabah) areas, West Khasi Hills District, Meghalaya, India. *J Environ Radioact* 99:1665–1670. <https://doi.org/10.1016/j.jenvrad.2008.04.014>
47. Sadasivan S, Shukla VK, Chinnaesakki S, Sartandel SJ (2003) Natural and fallout radioactivity measurement in Indian soils. *J Radioanal Nucl Chem* 256:603–607. <https://doi.org/10.1023/A:1024540925121>
48. Rahman MJJ, Faupl P, Alam MM (2009) Depositional facies of the subsurface Neogene Surma Group in the Sylhet Trough of the Bengal Basin, Bangladesh: record of tidal sedimentation. *Int J Earth Sci (Geol Rundsch)* 98:1971–1980. <https://doi.org/10.1007/s00531-008-0347-7>
49. Gazi MdY, Apu SI, Sharmili N, Rahman MdZ (2021) Origin and characterization of clay deposits in the Dupi Tila Formation of the Bengal Basin, Bangladesh. *Solid Earth Sci* 6:313–327. <https://doi.org/10.1016/j.sesci.2021.07.001>
50. Khanam F, Rahman MJJ, Abdullah R (2022) Clay minerals in interbedded sandstones and shales of the miocene surma group, sylhet trough, Bengal Basin (northeastern Indian Plate): implications for future hydrocarbon exploration. *Clays Clay Miner* 70:328–353. <https://doi.org/10.1007/s42860-022-00189-2>
51. Ahmed MM, Das SK, Haydar MA et al (2014) Study of natural radioactivity and radiological hazard of sand, sediment, and soil samples from inani beach, Cox's Bazar, Bangladesh. *J Nucl Part Phys* 4:69–78
52. Roy S, Hoque A (2001) Distribution of ¹³⁷Cs and naturally occurring radionuclides in soil at sites of the rooppur nuclear power plant
53. Miah F, Roy S, Touchiduzzaman M, Alam B (1998) Distribution of radionuclides in soil samples in and around Dhaka city. *Appl Radiat Isot* 49:133–137
54. Miah F, Molla MR, Alam M et al (1985) Exposure from natural sources of radiation. Report to the General Assembly, UN, New York, USA
55. Rahman M, Islam A, Kamal M, Chowdhury M (2012) Radiation hazards due to terrestrial radionuclides at the coastal area of Ship Breaking Industries, Sitakunda, Bangladesh. *Sci J Phys* 20(2):6
56. El-TaHER A, Zakaly HMH, Elsaman R (2018) Environmental implications and spatial distribution of natural radionuclides and heavy metals in sediments from four harbours in the Egyptian Red Sea coast. *Appl Radiat Isot* 131:13–22. <https://doi.org/10.1016/j.apradiso.2017.09.024>
57. Dai L, Wei H, Wang L (2007) Spatial distribution and risk assessment of radionuclides in soils around a coal-fired power plant: a case study from the city of Baoji, China. *Environ Res* 104:201–208. <https://doi.org/10.1016/j.envres.2006.11.005>
58. Yii MW, Wan Mahmood ZU, Ahmad Z et al (2011) NORM activity concentration in sediment cores from the Peninsular Malaysia East Coast Exclusive Economic Zone. *J Radioanal Nucl Chem* 289:653–661. <https://doi.org/10.1007/s10967-010-0928-3>
59. Tripathi R, Patra A, Mohapatra S et al (2013) Natural radioactivity in surface marine sediments near the shore of Vizag, South East India and associated radiological risk. *J Radioanal Nucl Chem* 295:1829–1835
60. Alaamer AS (2008) Assessment of human exposures to natural sources of radiation in Soil of Riyadh, Saudi Arabia. 6
61. Abbasi A, Mirekhtyari F (2020) Some physicochemical parameters and ²²⁶Ra concentration in groundwater samples of North Guilan. *Iran Atmosphere* 256:127113. <https://doi.org/10.1016/j.chemosphere.2020.127113>
62. Rudnick RL, Gao S (2014) Composition of the continental crust. *Treatise on geochemistry*. Elsevier, pp 1–51
63. Gupta S, Banerjee R, Babu PR et al (2012) Geochemistry of uraniumiferous Banganapalle sediments in the western part of Palnad Sub-basin, Andhra Pradesh: implications on provenance and paleoweathering. *Gond Geol Magz, Spec* 13:1–14
64. Okunlola OA, Idowu O (2012) The geochemistry of claystone-shale deposits from the Maastrichtian Patti formation. *Southern Bida basin, Nigeria*, p 12
65. Taylor SR, McLennan SM (1985) The continental crust: its composition and evolution
66. Clark SP, Peterman ZE, Heier KS (1966) Abundances of uranium, thorium, and potassium, handbook of physical constants, geological society of America. *Memoir* 97:521–541
67. Rogers J, Adams J (1969) Thorium. *Handb Geochem* 2:901–900
68. Ravisankar R, Vanasundari K, Suganya M et al (2014) Multivariate statistical analysis of radiological data of building materials used in Tiruvannamalai, Tamilnadu, India. *Appl Radiat Isot* 85:114–127. <https://doi.org/10.1016/j.apradiso.2013.12.005>
69. Tanasković I, Golobocanin D, Miljević N (2012) Multivariate statistical analysis of hydrochemical and radiological data of Serbian spa waters. *J Geochem Explor* 112:226–234
70. El Mamoney MH, Khater AEM (2004) Environmental characterization and radio-ecological impacts of non-nuclear industries on the Red Sea coast. *J Environ Radioact* 73:151–168. <https://doi.org/10.1016/j.jenvrad.2003.08.008>
71. Fares S (2017) Measurements of natural radioactivity level in black sand and sediment samples of the Tamsah Lake beach in Suez Canal region in Egypt. *J Radiat Res Appl Sci* 10:194–203. <https://doi.org/10.1016/j.jrras.2017.04.007>
72. Davis JC, Sampson RJ (1986) *Statistics and data analysis in geology*. Wiley, New York

Publisher's Note Springer Nature remains neutral with regard to jurisdictional claims in published maps and institutional affiliations.

Springer Nature or its licensor holds exclusive rights to this article under a publishing agreement with the author(s) or other rightsholder(s); author self-archiving of the accepted manuscript version of this article is solely governed by the terms of such publishing agreement and applicable law.